ELSEVIER
Available online at www.sciencedirect.com
SciVerse ScienceDirect
Physics Procedia 41 (2013) 266 – 275
Physics Procedia

Lasers in Manufacturing Conference 2013

UV-laser ablation of fibre reinforced composites with ns-pulses

H. Dittmar[a]*, F. Gäbler[b], U. Stute[a]

[a]*Laser Zentrum Hannover e.V., Hollerithallee 8, 30419 Hannover, Germany*
[b]*Coherent Inc., 5200 Patrick Henry Drive, 95054 Santa Clara, CA, USA*

Abstract

Within this work the ablation behaviour of both carbon and glass fibre reinforced epoxy resin was assessed when ablated by a nanosecond-pulsed laser source emitting radiation in the ultra-violet spectrum. The investigation focussed on the influences of pulse overlap, focus spot diameter and resulting fluence on process quality and machining time.
Results showed that ns-pulsed UV-lasers are capable of machining both types of fibre reinforced composites, while achieving good quality surfaces without burn marks or otherwise heat-damaged areas.

Keywords: laser ablation; composites; UV; ns; GFRP; CFRP

1. Motivation / State of the Art

Fibre reinforced composites gain significant importance in industrial product design. The wind energy industry has been utilising glass fibre reinforced plastics (GFRP) for years. In addition, the aeronautical industry is using carbon fibre reinforced plastics (CFRP) since the 1970s [Kjelgaard, 2012]. Recently, the automotive industry entered the CFRP market in order to use the lightweight benefits of reinforced plastics to reduce the fuel consumption of their products. As this development is expected to lead to a higher utilisation of CFRP, other material related challenges arise. While this includes the economic production of CFRP parts to satisfy the growing demand, focuses are also lying on recycling and repair strategies for those composites [Feraboli et al., 2012, Schulz and Saunders, 2012].

* Corresponding author. Tel.: +49 511 2788 335, Fax: +49 511 2788 100
E-mail address: h.dittmar@lzh.de

doi:10.1016/j.phpro.2013.03.078

Especially composite repair strategies involve conventional material processing techniques. Fibre reinforced plastics are a challenge to these techniques, due to their heterogeneous setup and in case of CFRP the hardness of the carbon fibres boosts tool wear, thus increasing processing costs.

Therefore, alternative processing strategies utilise lasers. Instead of conventional milling, pulsed laser radiation can be used to ablate material from large areas. As a non-contact tool the laser does not need to deal with material related tool-wear, nor is the process quality affected by the difference in stiffness of matrix material in comparison to the fibres. Concerning pulse duration, laser systems exist in ranges from microseconds to femtoseconds. It is understood that pulse duration affects two major aspects of laser processing: time and quality. Nanosecond (ns) pulsed systems are supposed to be a good compromise between the required quality and industrial relevant processing times. The process quality is also influenced by the chosen wavelength, with smaller wavelengths leading to better results [Takahashi et al., 2012].

While the laser has certain advantages, as mentioned above, compared to conventional milling machines, there are also some drawbacks. On the one hand, a laser process is heat-based. Therefore, processing strategies have to be optimised to not inflict heat-based damages [Dittmar et al., 2012, Niino and Kurosaki]. On the other hand, fibre reinforced plastics show different laser radiation transmission behaviours, which means that certain wavelengths are not utilisable to process particular fibres (e.g. glass fibres with near-infrared radiation).

Within this work it will be shown that ns-pulsed laser sources emitting radiation in the ultraviolet (UV) spectrum allow the ablation of both glass and carbon fibre reinforced plastics in industrial relevant processing times.

Nomenclature

i index (1 = 167mm objective, 2 = 255mm objective)
$d_{fs,i}$ focal spot diameter
$d_{ps,i}$ process spot diameter
$e_{l,i}$ energy per unit length
E_P pulse energy
f pulse repetition frequency
h_i hatch distance
$H_{P,i}$ fluence
L_i focal length
λ wavelength
$p_{d,x/y}$ pulse overlap (in x/y direction)
p_e effective pulse overlap
P_L laser output power
R_a surface roughness
t time
t_p pulse duration
V volume
v_i scanning velocity
v_0 scanning velocity at 0 % pulse overlap $p_{d,x/y}$

2. Experimental

The experiments were performed using a Coherent AVIA 355-23 emitting in the UV-spectrum at a wavelength of $\lambda = 355$ nm. The pulse repetition frequency can be varied between f = 10 kHz and f = 200 kHz. The laser's pulse duration is $t_p \leq 40$ ns for frequencies of up to f = 90 kHz. Maximum average laser output power is $P_L = 23.8$ W and maximum pulse energy is $E_P = 360$ µJ. The UV-laser beam is guided across the material by a galvanometer scanner with an exchangeable objective f-theta-lens and a focus shifter to vertically adjust the focus position. For the experiments performed, two different f-theta-lenses (focal lengths: $L_1 = 167$ mm and $L_2 = 255$ mm) were used in order to generate focal spots of different diameters.

The experiments were performed on two types of plastics. One was reinforced with glass fibres, the other one contained carbon fibres. Both CFRP and GFRP were non-crimped fabrics with unidirectional fibre orientation. The samples raw dimensions had been approximately 100x100 mm² with the GFRP having a thickness of about 10 mm and the CFRP being 4 mm thick.

Ablation is one of the major processes when it comes to the machining of fibre reinforced composites by laser as it can be used to remove large quantities of material, to alter surface properties and to drill. For bulk material removal, a defined area is filled with parallel lines, called hatch lines. Depending on the composite's build-up – whether it is a crimped or non-crimped fabric – different hatch strategies are applied.

In order to evaluate the laser's performance on different types of composites in terms of processing time and quality, both CFRP and GFRP were ablated on an area of 20x20 mm².

The trials for both materials were performed with a laser output power of $P_L = 23.6$ W, a pulse energy $E_P = 295$ µJ, a pulse repetition frequency of f = 80 kHz, and single-hatching. As already shown in earlier investigations [Völkermeyer et al.], the surface quality is depending not only on the process parameters, but also on the right hatch-strategy. Single-hatching means that the laser beam was guided only in a single direction. In this case it was guided perpendicular to the fibres' orientation to achieve good results. The focal plane was set at the top of the sample. The trials were performed twice per material utilising the very same process parameters but changing the objective. As this allowed to change the diameter of the focal spot d_{fs}, the fluence was altered. Objective 1 had a focal length of $L_1 = 167$ mm, which lead to a focal spot diameter of $d_{fs,1} = 20$ µm. Objective 2 with a focal length of $L_2 = 255$ mm provides a diameter of $d_{fs,2} = 48$ µm. Table 1 summarises the objective parameters.

Table 1. Objective parameters

parameter	unit	objective 1	objective 2
Focal length L_i	[mm]	167	255
Focal spot diameter $d_{fs,i}$	[µm]	20	48
Focal spot area	[mm²]	314 x 10^{-6}	1809 x 10^{-6}
Fluence $H_{P,i}$	[J/mm²]	0.94	0.16

To determine the effect of different pulse overlaps on the machining of fibre reinforced composites, the processing was performed with a pulse overlap in both x- and y-direction of $p_{d,x/y} = (-50, -25, 0, 25, 50)$ % in respect of the focal spot diameter $d_{fs,i}$. A negative pulse overlap means a distance between two single pulses that is bigger than the spot diameter $d_{fs,i}$. Therefore, the scanning velocity v_i and hatch-distance h_i were chosen according to the following equations (1) to (3), where v_0 is the scanning speed necessary for 0 % pulse overlap. Choosing pulse overlaps like this, leads to different energies per unit lengths, which are calculated according to equation (4).

$$f\, d_{fs,i} = v_0 \quad (1)$$
$$1 - p_{d,x} = v_i / v_0 \quad (2)$$
$$1 - p_{d,y} = h_i / d_{fs,i} \quad (3)$$
$$e_{l,i} = P_L / v_i \quad (4)$$

The following table 2 shows the machining parameters dependent on the pulse overlap.

Table 2. Machining parameters

pulse overlap	objective 1			objective 2		
$p_{d,x/y}$ [%]	v_1 [mm/s]	h_1 [µm]	$e_{l,1}$ [mJ/mm]	v_2 [mm/s]	h_2 [µm]	$e_{l,2}$ [mJ/mm]
50	800	10	29.50	1920	24	12.29
25	1200	15	19.67	2880	36	8.19
0	1600	20	14.75	3840	48	6.15
-25	2000	25	11.80	4800	60	4.92
-50	2400	30	9.83	5760	72	4.10

To demonstrate the ablation of bulk material, the aforementioned areas of 20x20 mm² were scanned with the laser 50 times. Afterwards, the focus was lowered by 2 mm using the focus shifter and the area was hatched for another 50 cycles.

3. Results

The experiments conducted on the samples made of CFRP and GFRP were evaluated with respect to processing time, amount of material removed, the ablated surfaces' roughness, and heat effects on the surrounding cutting edge.

Table 3 shows the time needed to hatch a field of 20x20 mm² during a single cycle dependent on the pulse overlap.

Table 3. Processing times per cycle

pulse overlap	objective 1	objective 2
$p_{d,x/y}$ [%]	t [s]	t [s]
50	65	15
25	32	8
0	20	5
-25	14	4
-50	11	3

The amount of material removed was determined by depth measurements relative to the surface of the specimen. The graphs in figure 1 show the energy needed to ablate one unit volume dependent on pulse overlap and fluence.

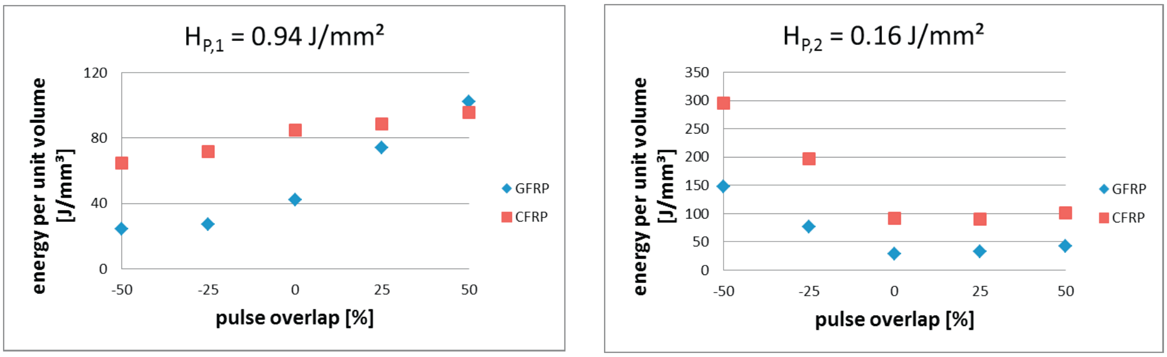

Fig. 1. Energy per unit volume necessary to remove material dependent on pulse overlap $p_{d,x/y}$ and the utilised fluencies

Comparing the results from fluencies $H_{P,1}$ and $H_{P,2}$, it can be seen that GFRP needs less energy to be removed. The rise of GFRP passed CFRP for overlaps $p_{d,x/y} > 25$ % is supposed to be linked to the massive melting and re-solidifying of the glass-fibres, eventually putting a constrain on the further material removal, leading to a higher amount of energy necessary to remove material. Apart from this, objective 1 shows that using a pulse overlap of $p_{d,x/y} < 0$ % is more effective to ablate fibre reinforced plastics (FRP), when high fluencies are used.

At a fluence of $H_{P,2}$, a pulse overlap of $p_{d,x/y} < 0$ % is not big enough to effectively ablate material, which is explained by the significantly lower fluence of $H_{P,2} = 0.16$ J/mm² compared to $H_{P,1} = 0.94$ J/mm². At this point both of the FRP are merely altered at the surface.

Investigating the amount of material removed per second, it can be seen that a fluence of $H_{P,1}$ allows the ablation of both FRP with a pulse overlap $p_{d,x/y} = -50$ %, whereas the fluence $H_{P,2}$ is not high enough to enable pulse distances in this range, resulting in a peak value for both tested materials at around $p_{d,x/y} = 0$ % (see figure 2).

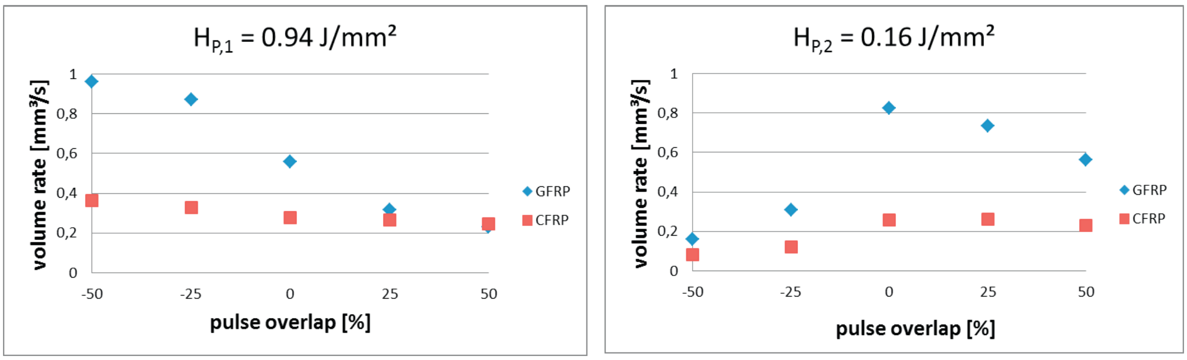

Fig. 2. Material removal rate dependent on pulse overlap $p_{d,x/y}$ and the utilised fluencies

The quality of the ablated surface was evaluated using a confocal microscope to measure the roughness of the surface. Figure 3 depicts the surface roughness for GFRP and CFRP

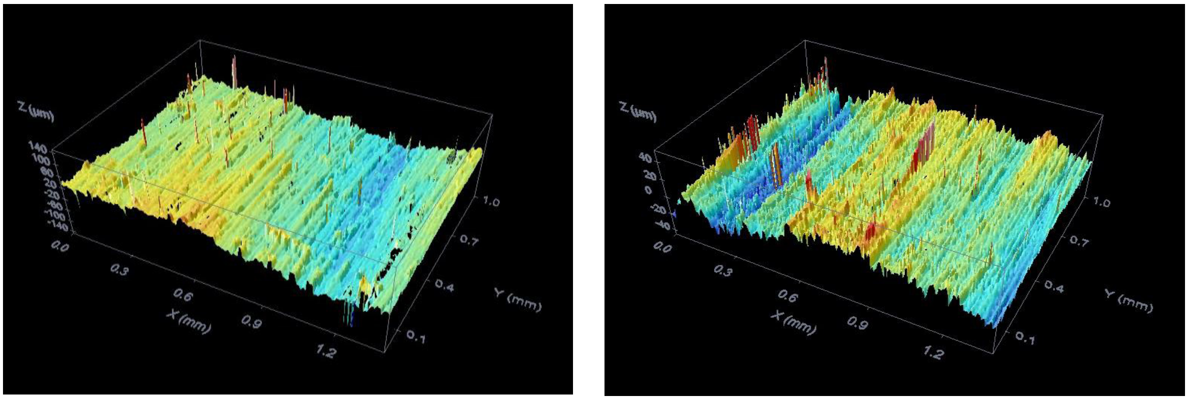

Fig. 3. Pictures showing surface topography of GFRP [$p_{d,x/y}$ = –50 %, $H_{P,1}$ = 0.94 J/mm²] (left) and CFRP [$p_{d,x/y}$ = 50 %, $H_{P,2}$ = 0.16 J/mm²] (right)

In order to measure the roughness of the ablated surfaces, the effective process spot diameter $d_{ps,i}$ was determined. While the laser beam's focal spot diameter $d_{fs,i}$ was used to calculate the pulse overlap, the material is influenced not only in this focal area, but also in areas adjacent to it. These side-effects have a direct influence on the surface roughness and thus need to be considered. Table 4 presents the process spot diameter for the tested materials at both fluencies $H_{P,1}$ and $H_{P,2}$.

Table 4. Process spot diameter $d_{ps,i}$

material	objective 1	objective 2
CFRP	50 µm	80 µm
GFRP	30 µm	60 µm

These process spot diameters $d_{ps,i}$ were used to re-evaluate the actual pulse overlap $p_{d,x/y}$. Therefore, for further discussion of the surface roughness the effective pulse overlap p_e based on the process spot diameter is used.

The results of the surface roughness measurements are depicted in figure 4 dependent on effective pulse overlap p_e. Comparing the surfaces' roughness, it needs to be differentiated between GFRP and CFRP in respect to fluence and pulse overlap. While for CFRP in general the differences between the roughness achieved with $d_{ps,1}$ and $d_{ps,2}$ was negligible, the GFRP surfaces were smoother when treated with the high fluence of $H_{P,1}$ = 0.94 J/mm² available at objective 1. The R_a = 530 µm at an effective pulse overlap of about p_e = 67 % (equals 50 % pulse overlap as in machining parameters, s. table 2) is not taken into account as this set of parameters lead to a molten and re-solidified surface with strong heat-affected zones. At a fluence of $H_{P,1}$ = 0.94 J/mm², no data was obtained for CFRP at an effective pulse overlap of p_e = 80 % (equals 50 % pulse overlap as in machining parameters, s. table 2), as this set of parameters ablated the 4-mm-thick material almost completely.

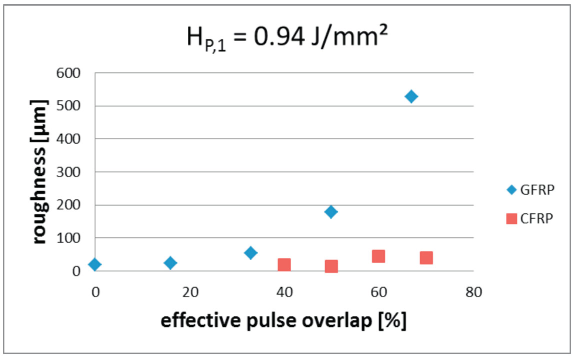

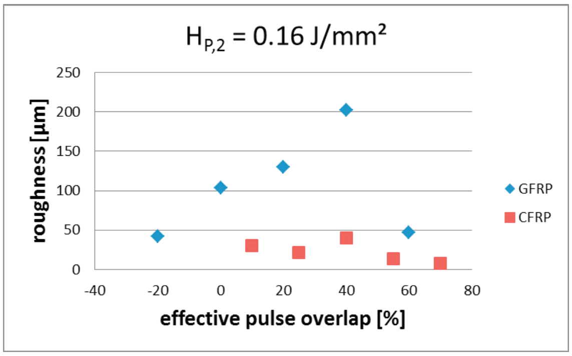

Fig. 4. Surface roughness dependent on effective pulse overlap p_e and the utilised fluencies

Using a fluence of $H_{P,1}$ both materials showed a lower surface roughness at low effective pulse overlaps p_e. Utilising fluence $H_{P,2}$ the results for surface roughness became better, when a higher effective pulse overlap p_e was chosen, although the graph for GFRP for $H_{P,2}$ suggests a different behaviour. But the performance of the objective 2 needs to be taken into account. As mentioned earlier in this article, the fluence of $H_{P,2}$ = 0.16 J/mm² was not high enough to effectively ablate the material with pulse overlaps p_e < 20 %, which is the reason, why the surface was almost unaffected (see figure 5). Figure 6 shows a GFRP surface processed with $H_{P,1}$ at an effective pulse overlap of p_e = 16 %.

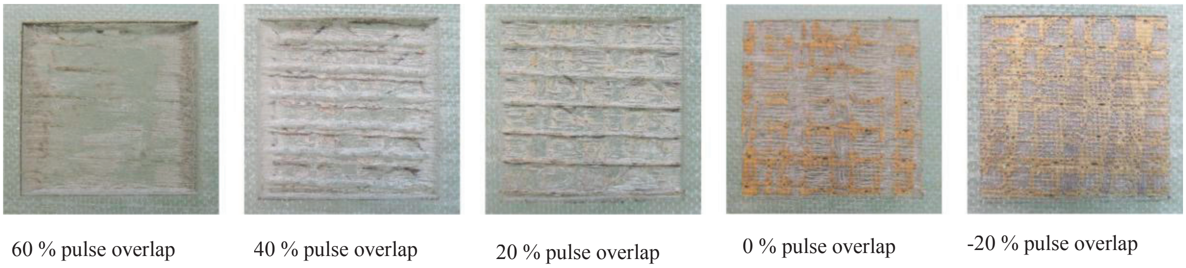

Fig. 5. Different GFRP surface qualities due to varying effective pulse overlaps p_e achieved with $H_{P,2}$

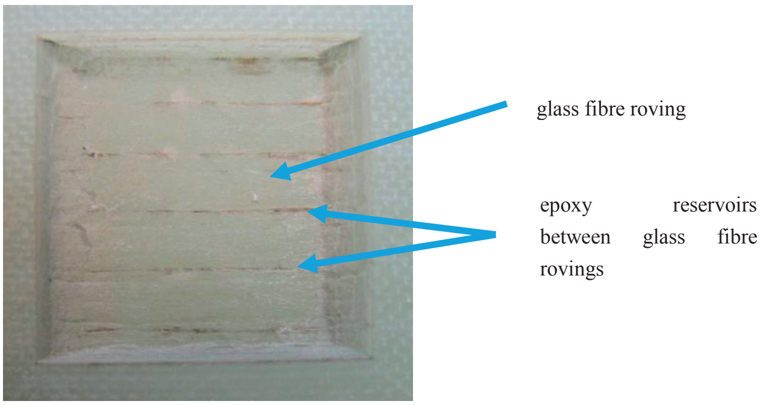

Fig. 6. Close-up view of a GFRP sample ablated with $H_{P,1}$ at p_e = 16 %

The visual inspection showed no burn-marks or heat-affected zones at the CFRP samples and at the GFRP treated with the lower fluence of $H_{P,2}$. The GFRP treated with the high fluence of $H_{P,1}$ was clearly affected by induced heat at pulse overlaps of $p_{d,x/y}$ = 0 % (machining parameters, s. table 2) and above resulting in sooty, burnt, or molten surfaces with extensive burn-marks at the cutting edges (see figure 7).

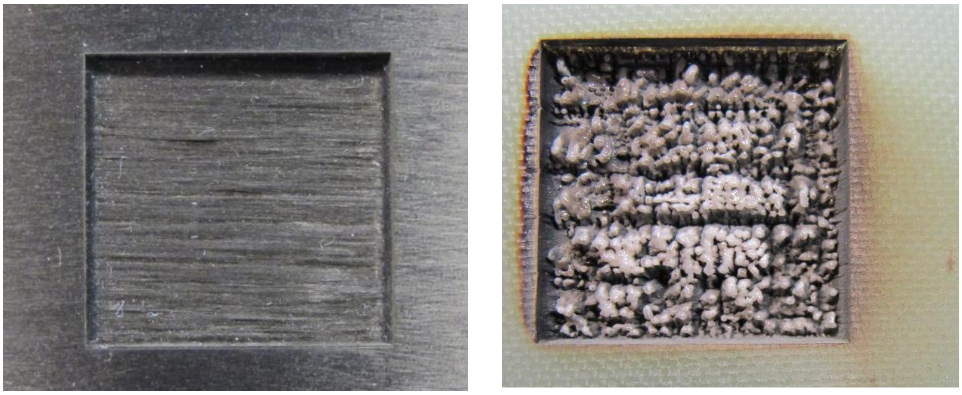

Fig. 7. CFRP at effective pulse overlap p_e = 70 % without any visible heat effects (left) and heat effects on GFRP at effective pulse overlap p_e = 67 % (right) using $H_{P,1}$ = 0.94 J/mm²

An analysis of the samples' cross-sections was also performed to identify possible damages, which could not be detected with visual inspection. For CFRP there were no damages detectable regardless of pulse overlap and fluence (see figure 8).

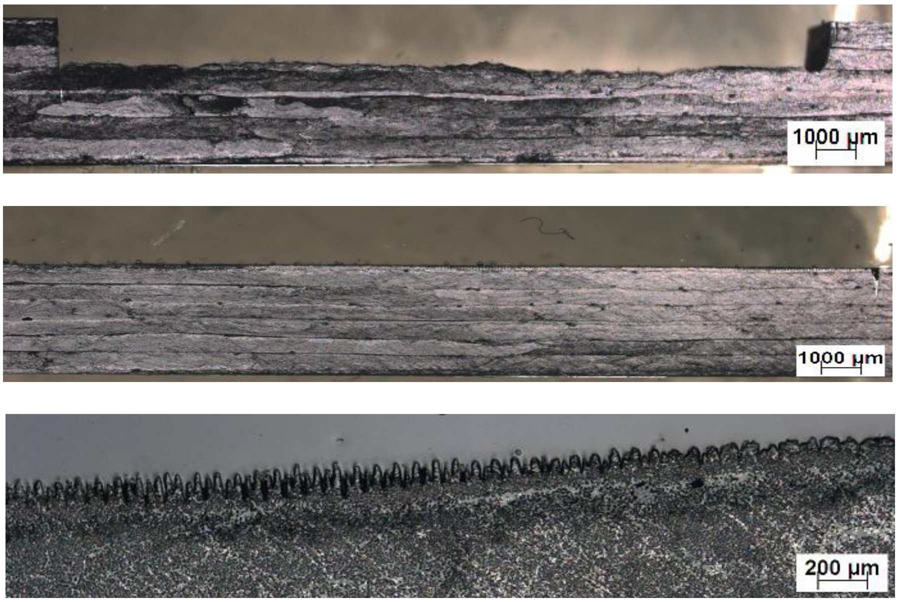

a) objective 1, 50 % effective pulse overlap — no damages identifiable

b) objective 2, 10 % effective pulse overlap — no damages identifiable

c) objective 2, 10 % effective pulse overlap — no damages identifiable

Fig. 8. Exemplary cross-sections of CFRP

A close-up view of the CFRP processed at $p_e = 10$ % effective pulse overlap reveals a spiky surface (see figure 8 b-c), which demonstrates that the laser's energy was high enough to ablate the CFRP at places, where pulses hit, but not high enough to remove material in the surrounding area.

The GFRP reacted to the induced heat by forming a heat affected zone at high pulse overlaps and high fluence. Whereas low pulse overlaps showed no signs of heat-based damages (see cross-sections depicted in figure 9).

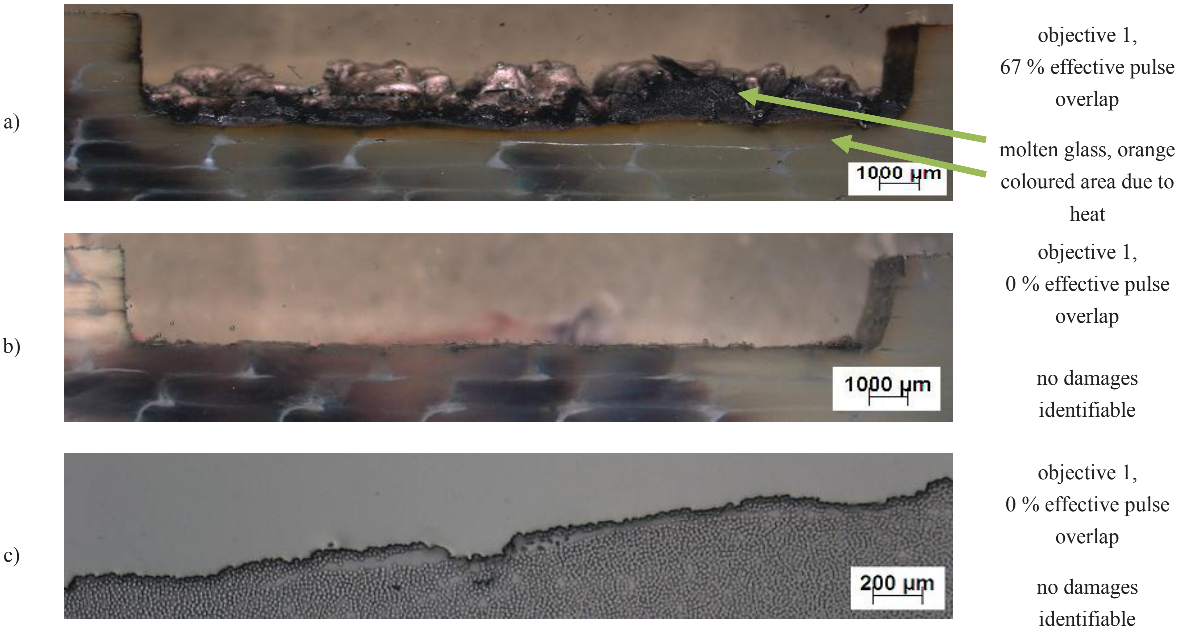

Fig. 9. Exemplary cross-sections of GFRP

4. Conclusion

The research presented showed that using an ns-pulsed UV-laser source allows for machining of both carbon and glass fibre reinforced plastics and it generated basic knowledge regarding the processing times and surface qualities achievable at different applied fluencies.

Using a fluence of $H_{P,1} = 0.939$ J/mm² (objective 1), V = 1 cm³ of GFRP were ablated in t = 18.3 min with a surface roughness of $R_a = 18.176$ µm, while the processing of CFRP reached a roughness of $R_a = 14.4$ µm at a total volume of V = 0.4 cm³ in t = 18.3 min. While this shows to be more effective in terms of processing time than utilising the fluence $H_{P,2} = 0.163$ J/mm² (CFRP: V = 0.348 cm³, t = 25 min, $R_a = 8.1$ µm; GFRP: V = 0.844 cm³, t = 25 min, $R_a = 47$ µm), a precise identification of this optimum needs to be done.

Also the influence of the pulse overlap on the process time needs to be investigated beyond this point. The high fluence of $H_{P,1}$ shows potential to further optimisation as the volume rate for GFRP might increase beyond 1 mm³/s for pulse overlaps $p_{d,x/y} < -50$ % (see fig.2).

While pulse overlap has its influence on processing time, it also affects the surface quality. Figure 4 showed that a low roughness can be achieved, when either using a high fluence and low pulse overlap or a high pulse overlap and low fluence. Therefore in terms of surface quality, optimal processing parameters are lying in between and have to be identified as well.

As it was shown, UV-lasers are capable of machining both FRP, but there are issues with high fluencies on GFRP as that might lead to molten glass, which negatively affects the surface roughness. Current UV-laser technology developments performed by Coherent, aim for a decrease in pulse duration. This is of interest to the machining of especially GFRP, since shorter pulses will reduce the necessity for higher fluences, thus avoiding molten glass in the working area. The Daytona 355-20 already provides 20W at 1 MHz with just 1 ns.

Acknowledgements

The authors would like to thank the German Federal Ministry for the Environment, Nature Conversation and Nuclear Safety (BMU), who supported part of this research presented with funding eurogia+ project ADVOCAT - Advanced Composite Repair Tooling for Wind Turbine Blade Maintenance (0325370).

References

Kjelgaard, C., 2012. Challenges in composites, Aircraft Technology 2012 116, p. 52.

Feraboli, P., Kawakami, H., Wade, B., Gasco, F., DeOto, L., Masini, A., 2012. Recyclability and reutilization of carbon fiber fabric/epoxy composites, Journal of Composite Materials 46, p. 1459.

Schulz, O.G., Saunders, P., 2012. "SLCR Laser Material Processing for Controlled Removal of CFRP as the first Step in the Repair Chain", Proceeding of SAMPE Tech, paper#2778.

Takahashi, K., Masuno, S., Tsukamoto, M., Nakai, K., Nariyama, T., Shinonaga, T., Nakano, H., Fujita, M., Abe, N., 2012. Study in the CFRP Processing with the High Harmonic Laser Light, Proceeding of International Symposium on Laser Processing of CFRP and Composites, paper#6-2.

Dittmar, H., Bluemel, S., Jaeschke, P., Stute, U., Kracht, D., 2012. "Advantages and Challenges of Laser Processing of CFRP with Ns-Pulses", Proceeding of International Congress on Applications of Lasers & Electro-Optics, paper#406.

Niino, H., Kurosaki, R., "Laser cutting of carbon fiber reinforced plastics (CFRP) by UV pulsed laser ablation", SPIE, http://dx.doi.org/10.1117/12.876231.

Völkermeyer, F., Jaeschke, P., Stute, U., Kracht, D., "Laser-based modification of wettability for carbon fiber reinforced plastics", Applied Physics A. DOI 10.1007/s00339-012-7237-3.